JPET Fast Forward. Published on December 2, 2009 as DOI: 10.1124/jpet.109.162313
JPET Fast Forward. Published on December 2, 2009 as DOI: 10.1124/jpet.109.162313
This article has not been copyedited and formatted. The final version may differ from this version.

JPET #162313

Title Page

Title: 2,2,2-Trichloroethanol activates a non-classical potassium channel in cerebrovascular smooth muscle and dilates the middle cerebral artery

Authors: Nikhil K. Parelkar, Ph.D., Neerupama Silswal, Ph.D., Kirsten Jansen, Joshua Vaughn, Robert M. Bryan Jr., Ph.D., Jon Andresen Ph.D.

Affiliations:

Basic Medical Science Department

Muscle Biology Research Group (MUBIG)

University of Missouri-Kansas City School of Medicine

Kansas City, MO 64108 (NKP, NS, KJ, JV, JA)

Department of Anesthesiology

Baylor College of Medicine

Houston, TX 77030 (RMB)

Downloaded from jpet.aspetjournals.org at ASPET Journals on March 13, 2024

Copyright 2009 by the American Society for Pharmacology and Experimental Therapeutics.

JPET Fast Forward. Published on December 2, 2009 as DOI: 10.1124/jpet.109.162313
This article has not been copyedited and formatted. The final version may differ from this version.

Running Title Page

Running title: Trichloroethanol dilates the MCA

Corresponding Author:

Jon Andresen, Ph.D.

Basic Medical Science Department

University of Missouri-Kansas City School of Medicine

2464 Charlotte St., HSB 2232

Kansas City, MO 64108

Office: 816-235-1883

Fax: 816-235-6517

andresenj@umkc.edu

Pages: 34

Figures: 7 + 1 supplementary figure

References: 35

Words: Abstract: 202

Introduction: 560

Discussion: 1170

Non-standard abbreviations: 2,2,2-trichloroethanol (TCE), extracellular K^+ $[K^+]_{out}$, currents due only to TCE (I_{TCE}), reversal potential (E_{rev}), inhibitory cocktail (IC)

Recommended section assignment: Cardiovascular

Downloaded from jpet.aspetjournals.org at ASPET Journals on March 13, 2024

JPET Fast Forward. Published on December 2, 2009 as DOI: 10.1124/jpet.109.162313
This article has not been copyedited and formatted. The final version may differ from this version.

Abstract

Trichloroacetaldehyde monohydrate (chloral hydrate (CH)) is a sedative/hypnotic that increases cerebral blood flow (CBF), and its active metabolite 2,2,2-trichloroethanol (TCE) is an agonist for the non-classical two-pore domain K^+ (K_{2P}) channels TREK-1 and TRAAK. We sought to determine if TCE dilates cerebral arteries *in vitro* by activating non-classical K^+ channels. TCE dilated pressurized and perfused rat middle cerebral arteries (MCAs) in a manner consistent with activation of non-classical K^+ channels. Dilation to TCE was inhibited by elevated external K^+ but not by an inhibitory cocktail (IC) of classical K^+ channel blockers. Patch clamp electrophysiology revealed that in the presence of the IC TCE increased whole-cell currents, and hyperpolarized the membrane potential of isolated MCA smooth muscle cells. Heating increased TCE sensitive currents indicating that the activated channel was thermosensitive. Immunofluorescence in sections of the rat MCA demonstrated that like TREK-1, TRAAK is expressed in the smooth muscle of cerebral arteries. Isoflurane did not, however, dilate the MCA suggesting that TREK-1 was not functional. These data indicate that TCE activated a non-classical K^+ channel with the characteristics of TRAAK in rat MCA smooth muscle cells. Stimulation of K^+ channels such as TRAAK in cerebral arteries may therefore partially explain how CH/TCE increases CBF.

Downloaded from jpet.aspetjournals.org at ASPET Journals on March 13, 2024

JPET Fast Forward. Published on December 2, 2009 as DOI: 10.1124/jpet.109.162313
This article has not been copyedited and formatted. The final version may differ from this version.

Introduction

Trichloroacetaldehyde monohydrate (chloral hydrate (CH)) is a sedative/hypnotic with a variety of uses ranging from sedation of agitated neonates to treatment of elderly patients with trouble sleeping (Pershad et al., 1999; Gauillard et al., 2002; Twite et al., 2004). CH is also used in veterinary medicine and in experimental animals although its use in humans and animals is declining (Cabana and Gessner, 1970; Gessner and Cabana, 1970; Silverman and Muir, 1993). The active metabolite of CH is 2,2,2-trichloroethanol (TCE) and both it and CH are environmental pollutants (Beland, 1999; Gauillard et al., 2002; NTP, 2002; Merdink et al., 2008). CH is rapidly metabolized to TCE in hepatocytes and erythrocytes but is only slowly excreted by the kidneys (Cabana and Gessner, 1970; Gessner and Cabana, 1970; Beland, 1999; Gauillard et al., 2002; NTP, 2002; Merdink et al., 2008). Thus, because of potentially life-threatening CNS depression, CH/TCE overdose is of concern (Gessner and Cabana, 1970; Levine et al., 1985; Jones and Singer, 2008).

The effects of CH/TCE on cerebral blood flow (CBF) are incompletely understood, however, CH appears to increase CBF. Using autoradiography, it was recently found that CH increased CBF and decoupled brain glucose metabolism from CBF (Uematsu et al., 2009). In addition, measurements of regional CBF using a tissue oxygen and glucose biosensor demonstrated that CH increased local CBF (Lowry and Fillenz, 2001). It is possible that the effects of CH/TCE on CBF are mediated by direct actions on cerebral arteries.

Downloaded from jpet.aspetjournals.org at ASPET Journals on March 13, 2024

JPET Fast Forward. Published on December 2, 2009 as DOI: 10.1124/jpet.109.162313
This article has not been copyedited and formatted. The final version may differ from this version.

By controlling the diameter of cerebral arteries, potassium (K^+) channels are determinants of CBF (Nelson and Quayle, 1995; Faraci and Heistad, 1998). Vascular smooth muscle cells (VSMC) express a variety of K^+ channels including classical and non-classical types, the later of which comprises the two-pore domain K^+ (K_{2P}) channel family (Nelson and Quayle, 1995; Faraci and Heistad, 1998; Lotshaw, 2007). Activation of K^+ channels in VSMC hyperpolarizes the cells promoting VSMC relaxation and thus vasodilation by closure of voltage-dependent calcium channels (Nelson and Quayle, 1995; Faraci and Heistad, 1998).

Interestingly, TCE is an agonist for the K_{2P} channels TREK-1 (KCNK2) and TRAAK (KCNK4), which are both expressed in cerebral arteries (Harinath and Sikdar, 2004; Bryan et al., 2006; Blondeau et al., 2007). TREK-1 is found throughout the wall of the mouse basilar artery (Blondeau et al., 2007), whereas the distribution of TRAAK in cerebral arteries has not been previously reported. Activation of heterologously expressed human TREK-1 by TCE was transient due to autoinhibition whereas stimulation of human TRAAK was sustained (Harinath and Sikdar, 2004). Although TCE activates K^+ channels that are expressed in cerebral arteries, the effect of TCE on cerebrovascular function has until now remained unexplored.

The purpose of this study was to examine the possibility that TCE is a vasodilator, and to determine the role of K^+ channels in the response to TCE. To address this, we studied *in vitro* pressurized and perfused rat middle cerebral arteries (MCAs) and found that TCE dilated these arteries in a manner consistent with activation of a non-classical K^+ channel. In addition, we used patch clamp electrophysiology to examine whole-cell currents in freshly dissociated rat MCA smooth muscle cells. TCE stimulated non-

Downloaded from jpet.aspetjournals.org at ASPET Journals on March 13, 2024

JPET Fast Forward. Published on December 2, 2009 as DOI: 10.1124/jpet.109.162313
This article has not been copyedited and formatted. The final version may differ from this version.

classical K^+ currents in, and hyperpolarized the membrane potential of MCA smooth muscle cells. Thus, our novel findings demonstrate that TCE activated a non-classical K^+ channel in cerebrovascular smooth muscle with characteristics of a K_{2P} channel, and dilated cerebral arteries.

Downloaded from jpet.aspetjournals.org at ASPET Journals on March 13, 2024

JPET Fast Forward. Published on December 2, 2009 as DOI: 10.1124/jpet.109.162313
This article has not been copyedited and formatted. The final version may differ from this version.

Methods

Animals and Reagents. Male Long-Evans rats (250-350 g) were purchased from Charles River (Wilmington, MA). Rats were anesthetized with 1-chloro-2,2,2-trifluoroethyl difluoromethyl ether (isoflurane, Abbott Laboratories, North Chicago, IL) and decapitated prior to tissue harvesting. The Animal Protocol Review Committee at Baylor College of Medicine or the Animal Care and Use Committee at the University of Missouri-Kansas City approved all protocols. All reagents were sourced from Sigma (St. Louis, MO) unless otherwise noted.

Western blotting. Rat tissue samples including the aorta, carotid arteries, cerebral arteries (MCA+basilar pooled from three rats), and heart were homogenized in protein extraction buffer (1% sodium monododecyl sulfate (SDS), 10 mM ethylenediaminetetraacetic acid (EDTA), and Complete mini protease inhibitor cocktail (Roche, Basel, CH)). Samples were heated to 85°C for 15 min and centrifuged at 15,000*g* for 15 min. Protein concentration of the supernatants was determined using the DC Protein Assay (BioRad, Hercules, CA). Samples were diluted with 6X Laemmeli buffer (30% glycerol, 50 mM EDTA, 0.25% bromophenol blue, and 10% β-mercaptoethanol) and heated to 85°C before loading 15 μg into wells of 4-20% polyacrylamide gels (Invitrogen, Carlsbad, CA). After room temperature electrophoresis at a constant 150 V, proteins were transferred to nitrocellulose membranes using the iBlot™ dry blotting system (Invitrogen) running program three for eight min. Blots were blocked for 1 hr using blocking solution (0.5% non-fat dry milk (BioRad), 1% bovine serum albumin (BSA), and 0.01%

Downloaded from jpet.aspetjournals.org at ASPET Journals on March 13, 2024

JPET Fast Forward. Published on December 2, 2009 as DOI: 10.1124/jpet.109.162313
This article has not been copyedited and formatted. The final version may differ from this version.

polysorbate 20 (Tween-20) in PBS (Invitrogen)) and then incubated overnight at 4°C with a primary goat polyclonal IgG directed against the C-terminus of human TRAAK (C-13, Santa Cruz Biotechnology, Santa Cruz, CA), which was diluted 1:100 in blocking solution.

Blots were then rinsed for 15 min three times at room temperature using 0.05% Tween-20 in PBS. After blocking for 1 hr blots were incubated for another hour with a fluorescently tagged (Alexa Fluor® 555, Invitrogen) rabbit anti-goat secondary antibody diluted 1:1000 in blocking solution. Blots were rinsed as before and the bands detected using an Ettan™ DIGE fluorescent imager (GE Healthcare Bio-Sciences, Piscataway, NJ).

Immunohistochemistry. Deeply anesthetized rats were decapitated, the brain was removed, and frozen in isopentane at -40°C, and sectioned at 8 μm using a cryostat. Sections were mounted two to a slide and fixed in 4% methanal (formaldehyde) for 10 min at room temperature. Slides were washed with 0.1% Triton X-100 in PBS (PBS-T), followed by blocking with 2% normal donkey serum and 10% BSA for 1 hour. Sections were incubated overnight at 4°C with either a rabbit anti-TRAAK antibody (BIOMOL, Plymouth Meeting, PA) at 8 ng ml^{-1} in blocking buffer, or an equivalent amount of rabbit non-immune IgG (Affinity Biologicals, Ancaster, ON Cananda) in blocking buffer as a control. On the second day, sections were thrice washed with PBS-T for 10 min each and then blocked for 1 hr. at room temperature. Sections were then incubated with a fluorescently tagged DyLight donkey anti-rabbit secondary antibody (Jackson ImmuoResearch, West Grove, PA) diluted 1:1000 in blocking buffer for 1 hr at room

Downloaded from jpet.aspetjournals.org at ASPET Journals on March 13, 2024

JPET Fast Forward. Published on December 2, 2009 as DOI: 10.1124/jpet.109.162313
This article has not been copyedited and formatted. The final version may differ from this version.

temperature. Following this, sections were incubated with 4',6-diamidino-2-phenylindole (DAPI, 1 μg/ml in blocking buffer) for 5 min. Prior to being cover-slipped, sections were washed three times in PBS-T, and dehydrated with increasing concentrations of ethanol. Sections were dried and coverslipped using VECTASHIELD HardSet mounting medium (Reactolab SA, Servion, CH).

Sections were imaged by epifluorescence microscopy using an Olympus IX51 inverted microscope (Center Valley, PA), Hamamatsu Orca-ERGA CCD camera (Bridgewater, NJ), Semrock Brightline DAPI and Texas Red filter sets (Rochester, NY), and X-cite 120 metal halide light source. Images were processed by Slide-Book imaging software (Intelligent Imaging Innovations, Denver, CO).

Isobaric vessel studies. Rat brains were quickly removed and placed in ice-cold Hank's buffered saline solution (HBSS, Invitrogen). The MCAs were carefully dissected away and studied in a pressurized artery myograph as previously described (Andresen et al., 2006). Briefly, isolated vessels were mounted on glass micropipettes, pressurized, and luminally perfused with Krebs buffer (in mM: 119 NaCl, 4.7 KCl, 24 $NaHCO_3$, 1.18 KH_2PO_4, 1.19 $MgSO_4$, 5.5 glucose, and 1.6 $CaCl_2$) bubbled with 20% O_2/5% CO_2/bal. N_2 at 37°C (pH=7.4). Endothelial denudation and verification was performed as previously described (Andresen et al., 2006). In these, and the following experiments, elevated external K^+ solutions were made isotonic by replacement of Na^+ with K^+ on an equimolar basis. Additionally, blockers of classical K^+ channels (10 mM tetraethylammonium (TEA) to block large conductance calcium activated K^+ (BK_{Ca}) channels, 100 μM $BaCl_2$ to block inwardly rectifying (K_{ir}) channels, 3 mM 4-pyridinamine (4-aminopyridine(4-

Downloaded from jpet.aspetjournals.org at ASPET Journals on March 13, 2024

JPET Fast Forward. Published on December 2, 2009 as DOI: 10.1124/jpet.109.162313
This article has not been copyedited and formatted. The final version may differ from this version.

AP)) to block voltage-gated K^+ (K_V) channels, and 10 μM 5-chloro-N-(4-[N-(cyclohexylcarbamoyl)sulfamoyl]phenethyl)-2-methoxybenzamide (glibenclamide) to block ATP-sensitive K^+ (K_{ATP}) channels) were added as an inhibitory cocktail (IC) 30 min prior to determining responses to various agonists in these and in subsequent experiments. Thus, by using these common, well accepted blockers, all types of classical K^+ channels should have been inhibited in our preparations (Nelson and Quayle, 1995). Any activation of a K^+ channel would therefore have had to be due to a non-classical K^+ channel, possibly a K_{2P} channel. All compounds, including TCE and the IC were added to the luminal and abluminal perfusates.

MCA digestion and smooth muscle cell isolation. Rat MCAs were removed from the brain and minced in digestion buffer (in mM: 135 NaCl, 5 KCl, 1.5 $MgCl_2$, 0.42 Na_2PO_4, 0.44 NaH_2PO_4, 4.2 $NaHCO_2$, 10 HEPES, and 1 mg/ml BSA with pH adjusted to 7.2 using 1.0 N NaOH). Enzymatic digestion started with a 37 min incubation at 37°C in digestion buffer containing 18 U/ml papain. After washing with digestion buffer, the digestion was completed by 8 min incubation at 37°C in digestion buffer containing 1.2 mg/ml collagenase II (Worthington Biochemical Corp., Lakewood, NJ), 0.8 mg/ml soybean trypsin inhibitor (Worthington Biochemical Corp.), and 60 U/ml elastase (EMD Chemicals, Gibbstown, NJ). Dissociated tissue was twice washed in digestion buffer and then triturated by passing the digest 10 times through the tip of a 200 μl pipette tip pre-coated with digestion buffer containing BSA. The MCA tissue digest was stored on ice until use during the same day.

Downloaded from jpet.aspetjournals.org at ASPET Journals on March 13, 2024

JPET Fast Forward. Published on December 2, 2009 as DOI: 10.1124/jpet.109.162313
This article has not been copyedited and formatted. The final version may differ from this version.

Electrophysiology. Aliquots (~20 μl) of the rat MCA smooth muscle cell suspension were placed in the well of a laminar perfusion chamber (Bioscience Tools, San Diego, CA) on the stage of an IX71 inverted microscope (Olympus, Center Valley, PA) and the cells allowed to attach to the glass for 10 min before initiating buffer flow. Smooth muscle cells were superfused with bath buffer (in mM: 140 NaCl, 4.2 KCl, 3 $NaHCO_3$, 1.2 KH_2PO_4, 2 $MgCl_2$, 0.1 $CaCl_2$, 10 glucose, 10 2-[4-(2-hydroxyethyl)piperazin-1-yl]ethanesulfonic acid (HEPES) with pH adjusted to 7.4 using 1.0 N NaOH) at ~1 ml/min. As is typical for patch clamp studies, experiments were performed at room temperature (RT) unless otherwise noted and solutions were not aerated. Micropipettes were made from Warner Instruments (Hamden, CT) 8520 glass capillaries using a Narishige (East Meadow, NY) PC-10 gravity puller. Micropipettes were polished to 3-5 MΩ resistance with a Narishige MF-830 microforge and filled with pipette buffer (in mM: 140 KCl, 1.0 $MgCl_2$, 2.2 $CaCl_2$, 3 glycol-bis(2-aminoethylether)-N,N,N′,N′-tetraacetic acid ((EGTA): results in ~0.42 μM free Ca^{2+}), and 10 HEPES with pH adjusted to 7.2 using 1.0 N KOH). Osmolarity of bath and pipette solutions was measured using a Wescor (Logan, UT) VAPRO™5520 vapor pressure osmometer and adjusted to 285 mOsmol/L if necessary.

Gentle suction was used to form gigiseals on individual smooth muscle cells, and further suction ruptured the membrane inside the pipette tip to form the whole-cell patch clamp configuration. A MultiClamp 700B computer-controlled microelectrode amplifier and DigiData1440A low-noise digitizer run by pCLAMP 10 software (v10.2.0.14, Axon Instruments, Union City, CA) were used to acquire and measure the whole-cell currents. Holding potential was -20 mV. Current-voltage (I-V) plots were generated from a

Downloaded from jpet.aspetjournals.org at ASPET Journals on March 13, 2024

JPET Fast Forward. Published on December 2, 2009 as DOI: 10.1124/jpet.109.162313
This article has not been copyedited and formatted. The final version may differ from this version.

voltage-step protocol that increased membrane potential from -80 mV to +80 mV in 10 mV steps. Three consecutive traces were averaged to generate each I-V profile. The temperature of the recording chamber was changed using a TC-1 temperature controller (Bioscience Tools), which received feedback from a thermocouple placed in the recording chamber. RT averaged ~22°C, and for heat experiments bath temperature was raised to 33°C in less than one min. For experiments involving K^+ channel blockade, the IC of classical K^+ channel blockers was added to the bath buffer and pH adjusted to 7.4 with 1.0 N NaOH. Voltage ramps (-100 mV to +100 mV over 700 ms) were used to probe reversal potential (E_{rev}) changes in solutions of varying K^+ concentration. As above, three consecutive traces were averaged to generate each I-V profile. In solutions with elevated external K^+ ($[K^+]_{out}$), an equal amount of Na^+ was removed to maintain osmotic balance. The pH of 140 mM K^+ was adjusted to 7.4 with 1.0 N KOH. Membrane potentials were recorded in current-clamp mode. For all experiments, liquid junction potential adjustments were made during data analysis.

Statistics. Data are plotted and expressed as means ± SEM. N-values are detailed in the legends to the figures where each n-unit represents data from one animal. In isobaric arterial studies one artery was studied from each animal. Changes in the diameter of pressurized and perfused arteries were calculated as previously described (Andresen et al., 2006). Electrophysiological data represent an average of at least three cells per animal (range is 3-6 cells/animal). Statistics were computed by comparing responses across animals. Two-factor ANOVA was used to determine differences between concentration-response curves. One-factor ANOVA with Tukey's multiple comparison *post-hoc* tests or

Downloaded from jpet.aspetjournals.org at ASPET Journals on March 13, 2024

JPET Fast Forward. Published on December 2, 2009 as DOI: 10.1124/jpet.109.162313
This article has not been copyedited and formatted. The final version may differ from this version.

a paired Student's t-test as appropriate were used to compare peak outward currents. Changes in membrane potential under current-clamp were compared with a paired Student's t-test. Where appropriate, data normality was examined with D'Agostino and Pearson tests and homogeneity of variance was determined with Bartlett's test. To determine differences between I-V relationships, the data were fitted with third order polynomial functions and the best-fit lines compared by extra sum-of-squares F-test. Data were plotted and statistics computed with Graphpad Prism® (v5.0b, San Diego, CA). Significance was accepted at $p \leq 0.05$.

Downloaded from jpet.aspetjournals.org at ASPET Journals on March 13, 2024

JPET Fast Forward. Published on December 2, 2009 as DOI: 10.1124/jpet.109.162313
This article has not been copyedited and formatted. The final version may differ from this version.

Results

Vascular Responses to TCE and isoflurane

Initial experiments demonstrated that TCE dilated intact rat MCAs and that endothelial denudation did not alter the dilation (data not shown). Thus, to examine just the effect of TCE on smooth muscle, experiments were conducted on denuded MCAs. Figure 1 (top) shows raw traces illustrating the response of pressurized and perfused rat MCAs to increasing concentrations of TCE. Under control conditions, TCE caused concentration-dependent ($p<0.0001$) dilation of rat MCA (figure 1A). Figure 1B demonstrates that elevating $[K^+]_{out}$ to 60 mM substantially impaired ($p<0.0001$) the dilation to TCE. We next added the IC of classical K^+ channel blockers to explore the identity of the K^+ channel(s) involved in the dilation to TCE. As can be seen in figure 1C, the IC did not alter ($p=0.7821$) the dilation to TCE in the rat MCA. In separate experiments, application of increasing concentrations (10^{-5} to 10^{-1} M) of isoflurane totally failed to dilate denuded, pressurized and perfused rat MCAs (data not shown).

In addition to the MCA, we found that TCE also dilated pressurized and perfused rat carotid arteries. Supplemental figure 1 shows that TCE concentration-dependently ($p<0.0001$) dilated the rat carotid, and that like the MCA, elevated $[K^+]_{out}$ but not the IC impaired ($p<0.0001$) the dilation.

TRAAK Expression

Downloaded from jpet.aspetjournals.org at ASPET Journals on March 13, 2024

JPET Fast Forward. Published on December 2, 2009 as DOI: 10.1124/jpet.109.162313
This article has not been copyedited and formatted. The final version may differ from this version.

We found an immunopositive band for TRAAK near 43 kDa (predicted TRAAK size) in the rat MCA by Western blot (figure 2A). In addition, we found that TRAAK was expressed in hearts, aortas, and the carotid arteries of rats (figure 2A). We further investigated the expression of TRAAK in the vascular wall of the rat MCA by immunohistochemistry. In 8 μm rat brain sections containing the MCA TRAAK immunoreactivity was visible in neurons and in the MCA (figure 2B). At high magnifications TRAAK expression appeared to be restricted to the smooth muscle layers of the MCA.

Downloaded from jpet.aspetjournals.org at ASPET Journals on March 13, 2024

Electrophysiology of MCA smooth muscle: Response to TCE under control conditions

Figure 3 shows raw traces of the responses of individual rat MCA vascular smooth muscle cells responding to a voltage step stimulus protocol at baseline, and after exposure to TCE. In both control myocytes and in those treated with the IC, inward current was characteristically small for rat MCA smooth muscle cells (Bryan et al., 2006). Under control conditions, TCE increased whole-cell currents primarily in the outward direction at depolarizing potentials (currents going upwards in figure 3 and figure 4B&C). Control outward current at 60 mV was significantly greater ($p=0.0005$) than baseline only at 10^{-2} M TCE (figure 4A), yet, TCE concentration-dependently ($p<0.0001$ [the entire curve]) increased overall whole-cell currents in the control condition (figure 4B). Subtracting out the baseline response to generate difference currents revealed the currents due only to TCE (I_{TCE}). In the control condition I_{TCE} (figure 4C) reversed at about -45 mV for both 10^{-3} and 10^{-2} M TCE, which was hyperpolarized

JPET Fast Forward. Published on December 2, 2009 as DOI: 10.1124/jpet.109.162313
This article has not been copyedited and formatted. The final version may differ from this version.

compared to E_{rev} at baseline (~ -36 mV). Peak I_{TCE} at 10^{-2} M TCE was nine-fold greater than I_{TCE} at 10^{-3} M TCE (figure 4C).

Electrophysiology of MCA smooth muscle: Response to TCE after blockade of classical K^+ channels

Currents at 60 mV stimulated by TCE in the control condition were reduced by 80% at 60 mV after addition of the IC, suggesting that classical K^+ channels were responsible for much of the control response to TCE (figure 3 and 4B). Unlike the control condition, after addition of the IC inward currents were increased by TCE (figures 3A and 4B). In the presence of the IC, 10^{-2} M, but not 10^{-3} M TCE increased ($p=0.0144$) outward current at 60 mV over baseline levels (figure 4A). Likewise, only 10^{-2} M TCE increased ($p<0.0001$) the total response (entire I-V curve) over baseline levels in the presence of the IC (figure 4B). Subtracting out the baseline response revealed the currents due only to TCE in the presence of the IC ($I_{TCE(IC)}$). As expected from the summary data in figure 4B, the difference currents demonstrated that $I_{TCE(IC)}$ for 10^{-3} M TCE was essentially zero at every voltage, meaning that it was indistinguishable from baseline currents. $I_{TCE(IC)}$ at 10^{-2} M TCE was, however, significantly ($p<0.0001$) non-zero and did not display voltage sensitivity (figure 4C). E_{rev} for $I_{TCE(IC)}$ at 10^{-2} M TCE was about -24 mV (figure 4C). While not a large shift, this was hyperpolarized compared to baseline (E_{rev} about -21mV). To address this more carefully we switched to current-clamp mode, which allowed for direct determination of the cell membrane potential. In the presence of

Downloaded from jpet.aspetjournals.org at ASPET Journals on March 13, 2024

JPET Fast Forward. Published on December 2, 2009 as DOI: 10.1124/jpet.109.162313
This article has not been copyedited and formatted. The final version may differ from this version.

the IC, 10^{-2} M TCE hyperpolarized (p=0.0085) the membrane potential by 12±3 mV (-25±1.2 mV to -37±3.4 mV, N=5).

Changes in reversal potential with increased extracellular potassium

Experimental data from rat MCA smooth muscle cells demonstrated a positive shift in E_{rev} with increasing $[K^+]_{out}$ as expected if the charge carrier was K^+ (figure 5). In normal bath buffer (5.4 mM K^+_{out}) currents stimulated by 10^{-2} M TCE in the presence of the IC reversed around -32 mV. Increasing $[K^+]_{out}$ to 54 and 140 mM shifted E_{rev} to -17 and -1 mV respectively. Figure 5 (bottom) shows the best-fit lines through the summary data our experimental results in addition to a simulated data set based on a hypothetical pure K^+ current. The slope of the best-fit line for the experimental data was 19.98±2 mV/decade, which is less (p<0.0001) than the predicted 59.65±2 mV/decade for a pure K^+ current.

Effect of heat on the TCE response

In the presence of the IC, simply heating the patch chamber did not increase baseline whole-cell currents (figure 6). Heating to 33°C in the presence of 10^{-3} M TCE and the IC, however, increased (p<0.0001) whole-cell currents above those present at RT such that the outward current at 60 mV and 33°C was 1.7-fold greater (p=0.0195) than RT levels (figure 7A-C). Examining the difference currents ($I_{TCE(IC)}$) revealed that TCE currents at 33°C were greater (p=0.0001, entire curve) than those at RT (figure 7D). In

Downloaded from jpet.aspetjournals.org at ASPET Journals on March 13, 2024

JPET Fast Forward. Published on December 2, 2009 as DOI: 10.1124/jpet.109.162313
This article has not been copyedited and formatted. The final version may differ from this version.

addition, $I_{TCE(IC)}$ at 10^{-2} M TCE and RT were indistinguishable ($p=0.2842$) from $I_{TCE(IC)}$ stimulated by just 10^{-3} M TCE at 33° C (figure 7E).

Downloaded from jpet.aspetjournals.org at ASPET Journals on March 13, 2024

JPET Fast Forward. Published on December 2, 2009 as DOI: 10.1124/jpet.109.162313
This article has not been copyedited and formatted. The final version may differ from this version.

Discussion

For the first time we have observed that TCE elicited endothelium-independent dilation of the rat MCA in a manner consistent with the activation of a non-classical K^+ channel. We found that the TCE sensitive K_{2P} channel TRAAK was expressed in the smooth muscle layers of the MCA. In isolated MCA smooth muscle cells, TCE caused hyperpolarization and increased whole-cell currents apparently by stimulating a non-classical K^+ channel. In addition, heat potentiated the TCE response in MCA smooth muscle cells in the presence of the IC, which is compatible with activation of a thermosensitive channel such as TRAAK. Thus, it appears that TCE causes vasodilation by activating non-classical K^+ channels, possibly the K_{2P} channel TRAAK.

Vasomotor function

In control MCAs 10^{-3} M TCE caused 13% dilation and at $10^{-1.5}$ M TCE 100% dilation was reached. The dilation we observed to TCE was endothelium-independent and largely inhibited by elevated extracellular K^+. Elevated extracellular K^+ alters the equilibrium potential for K^+, thereby reducing the driving force for K^+ movement across the cell membrane. Thus, these data indicated that some type of K^+ channel was involved in the response. Addition of the IC did not, however, impair the response of the rat MCA or carotid artery to TCE indicating involvement of a non-classical K^+ channel, possibly a K_{2P} channel since they are refractory to known K^+ channel blockers. These data are

Downloaded from jpet.aspetjournals.org at ASPET Journals on March 13, 2024

JPET Fast Forward. Published on December 2, 2009 as DOI: 10.1124/jpet.109.162313
This article has not been copyedited and formatted. The final version may differ from this version.

similar to previous work showing that the rat MCA dilated to the AA by activation of a non-classical K^+ channel in an endothelium-independent manner (Bryan et al., 2006).

Because TREK-1&-2 are expressed in the rat MCA, it was necessary to evaluate TREK-1 as a possible mediator of the dilatory response to TCE since TCE can activate both TREK-1&-2 and TRAAK. The TREK channel agonist and inhalation anesthetic, isoflurane, failed to elicit any dilation of rat MCAs suggesting that TREK-1&-2 were not functionally present in our preparations. Furthermore, although TCE is an agonist for TREK-1 (there are no published data for TREK-2) and TRAAK, activation of TREK-1 by TCE is transient because of rapid channel inhibition (Harinath and Sikdar, 2004). The dilatory response to TCE, however, was sustained further supporting the involvement of TRAAK rather than TREK-1 channels in pressurized and perfused arteries.

TRAAK Expression

Initially, TRAAK message was found only in the brain, spinal cord, and retina (Fink et al., 1998; Reyes et al., 2000). Subsequently, we found TRAAK message and protein and rat cerebral arteries (Bryan et al., 2006). The present study extends these findings by demonstrating that TRAAK protein is expressed in rat carotid arteries, aortas and heart. Since TRAAK was also found in rat mesenteric, but not in pulmonary arteries TRAAK, therefore, appears to be generally expressed in the cardiovascular system, at least in the systemic circulation (Gardener et al., 2004). The expression of TRAAK in the wall of the rat MCA appeared to be restricted to the smooth muscle layers as we did not observe TRAAK immunofluorescence in endothelial cells. Although our images do not

Downloaded from jpet.aspetjournals.org at ASPET Journals on March 13, 2024

JPET Fast Forward. Published on December 2, 2009 as DOI: 10.1124/jpet.109.162313
This article has not been copyedited and formatted. The final version may differ from this version.

totally exclude the possibility that TRAAK is expressed in endothelium, our functional data both in the present work, and in our previous study, suggests that TRAAK is functionally present only in vascular smooth muscle.

Electrophysiology

The currents stimulated by TCE in control conditions were large, and had a distinct voltage-dependent component. Addition of the IC substantially reduced the overall response to TCE but in so doing revealed voltage-independent currents attributable to a non-classical K^+ channel. Given that the large voltage-dependent current stimulated by TCE was IC-sensitive, it is most likely that large conductance calcium-activated K^+ channels (BK_{Ca}) carried these currents. Although potentially interesting, we did not pursue this further because our pressurized and perfused *in vitro* artery data did not support a role for BK_{Ca} channels in the response to TCE.

In order to examine if K^+ carried I_{TCE} we increased $[K^+]_{out}$ in order to determine E_{rev} as a proxy for the cell membrane potential. In the presence of 10^{-2} M TCE the shifts in E_{rev} caused by 54 and 140 mM K^+_{out} were as expected if K^+ was the current carrier, in the normal buffer (5.4 mM K^+_{out}) E_{rev} was not as hyperpolarized as one might expect if there was sole activation of only a K^+-selective channel. This suggests that TCE activated not only K^+ currents, but also other cationic currents that tended to shift E_{rev} to more positive values. It was, however, *a priori* unlikely that TCE would be totally specific for a particular ion channel. For example, TCE altered calcium handling in rat submandibular acinar cells, and inhibited NMDA receptors in neurons (Scheibler et al., 1999; Fischer et

Downloaded from jpet.aspetjournals.org at ASPET Journals on March 13, 2024

JPET Fast Forward. Published on December 2, 2009 as DOI: 10.1124/jpet.109.162313
This article has not been copyedited and formatted. The final version may differ from this version.

al., 2000; Pochet et al., 2002). Even though TCE apparently activated cation channels other than K^+ channels, the net effect of TCE in the MCA was vasodilation, which is best explained by a predominance of K^+ channel activation. The present results are, however, similar to the ~38 mV/decade slope we previously demonstrated in isolated rat MCA smooth muscle cells responding to 10^{-5} M AA (Bryan et al., 2006).

Using current-clamp mode to determine the membrane potential directly, we found that 10^{-2} M TCE hyperpolarized MCA smooth muscle cells by 12 mV. Again, this is best explained by activation of a K^+ channel because under the experimental conditions K^+ is the only ion whose equilibrium potential lay negative to the resting membrane potential. A hyperpolarization of 12 mV is large enough to cause substantial relaxation of the rat MCA (Knot and Nelson, 1998; Marrelli et al., 2003). Thus, these data support the conclusion that TCE dilates the MCA by stimulating a non-classical K^+ channel.

We found that heat increased TCE sensitive whole-cell currents two-fold. Indeed, heating to 33°C in the presence of 10^{-3} M TCE elicited currents virtually identical to those stimulated by 10^{-2} M TCE at RT. This is exactly the type of enhanced response one might expect if two or more stimuli converged upon a common target. In COS-7 cells overexpressing recombinant TRAAK, heating above 25°C stimulated TRAAK channel currents reaching a maximum activation at 42°C (Kang et al., 2005). These data, therefore, support the conclusion that TCE activated a thermosensitive non-classical K^+ channel, possibly TRAAK, in isolated rat MCA smooth muscle cells. Although whole-cell patches of MCA smooth muscle cells became unstable above 33°C, it is possible that elevating the temperature beyond this point would have further increased TCE-sensitive currents.

Downloaded from jpet.aspetjournals.org at ASPET Journals on March 13, 2024

JPET Fast Forward. Published on December 2, 2009 as DOI: 10.1124/jpet.109.162313
This article has not been copyedited and formatted. The final version may differ from this version.

Summary and Significance

Doses of CH that do not cause sedation can result in plasma TCE concentrations of ~30 μM whereas sedative doses may elevate TCE into the mM range (Beland, 1999; Pochet et al., 2002; Merdink et al., 2008). Thus, stimulation of non-classical K^+ channels to cause vasodilation may be clinically relevant. Although we are limited by a lack of specific pharmacology, and the current unavailability of TRAAK knockout mice, based on current knowledge of the ion channels expressed in vascular smooth muscle, and on the activation pattern of the channels stimulated by our interventions, it is possible that TRAAK may be capable of modulating the diameter of cerebral arteries.

Downloaded from jpet.aspetjournals.org at ASPET Journals on March 13, 2024

JPET Fast Forward. Published on December 2, 2009 as DOI: 10.1124/jpet.109.162313
This article has not been copyedited and formatted. The final version may differ from this version.

Acknowledgements

The authors would like to thank Sean Marrelli Ph.D. and Michael Wacker Ph.D. for valuable advice and technical support.

Downloaded from jpet.aspetjournals.org at ASPET Journals on March 13, 2024

JPET Fast Forward. Published on December 2, 2009 as DOI: 10.1124/jpet.109.162313
This article has not been copyedited and formatted. The final version may differ from this version.

References

Andresen JJ, Shafi NI, Durante W and Bryan RM, Jr. (2006) Effects of carbon monoxide and heme oxygenase inhibitors in cerebral vessels of rats and mice. *Am J Physiol Heart Circ Physiol* **291**:H223-230.

Beland FA (1999) NTP technical report on the toxicity and metabolism studies of chloral hydrate (CAS No. 302-17-0). Administered by gavage to F344/N rats and B6C3F1 mice. *Toxic Rep Ser*:1-66, A61-E67.

Blondeau N, Petrault O, Manta S, Giordanengo V, Gounon P, Bordet R, Lazdunski M and Heurteaux C (2007) Polyunsaturated fatty acids are cerebral vasodilators via the TREK-1 potassium channel. *Circ Res* **101**:176-184.

Bryan RM, Jr., You J, Phillips SC, Andresen JJ, Lloyd EE, Rogers PA, Dryer SE and Marrelli SP (2006) Evidence for two-pore domain potassium channels in rat cerebral arteries. *Am J Physiol Heart Circ Physiol* **291**:H770-780.

Cabana BE and Gessner PK (1970) The kinetics of chloral hydrate metabolism in mice and the effect thereon of ethanol. *J Pharmacol Exp Ther* **174**:260-275.

Faraci FM and Heistad DD (1998) Regulation of the cerebral circulation: role of endothelium and potassium channels. *Physiol Rev* **78**:53-97.

Fink M, Lesage F, Duprat F, Heurteaux C, Reyes R, Fosset M and Lazdunski M (1998) A neuronal two P domain K+ channel stimulated by arachidonic acid and polyunsaturated fatty acids. *Embo J* **17**:3297-3308.

Downloaded from jpet.aspetjournals.org at ASPET Journals on March 13, 2024

JPET Fast Forward. Published on December 2, 2009 as DOI: 10.1124/jpet.109.162313
This article has not been copyedited and formatted. The final version may differ from this version.

Fischer W, Allgaier C and Illes P (2000) Inhibition by chloral hydrate and trichloroethanol of AMPA-induced Ca(2+) influx in rat cultured cortical neurones. *Eur J Pharmacol* **394**:41-45.

Gardener MJ, Johnson IT, Burnham MP, Edwards G, Heagerty AM and Weston AH (2004) Functional evidence of a role for two-pore domain potassium channels in rat mesenteric and pulmonary arteries. *Br J Pharmacol* **142**:192-202.

Gauillard J, Cheref S, Vacherontrystram MN and Martin JC (2002) [Chloral hydrate: a hypnotic best forgotten?]. *Encephale* **28**:200-204.

Gessner PK and Cabana BE (1970) A study of the interaction of the hypnotic effects and of the toxic effects of chloral hydrate and ethanol. *J Pharmacol Exp Ther* **174**:247-259.

Harinath S and Sikdar SK (2004) Trichloroethanol enhances the activity of recombinant human TREK-1 and TRAAK channels. *Neuropharmacology* **46**:750-760.

Honore E, Patel AJ, Chemin J, Suchyna T and Sachs F (2006) Desensitization of mechano-gated K2P channels. *Proc Natl Acad Sci U S A* **103**:6859-6864.

Jones GR and Singer PP (2008) An unusual trichloroethanol fatality attributed to sniffing trichloroethylene. *J Anal Toxicol* **32**:183-186.

Kang D, Choe C and Kim D (2005) Thermosensitivity of the two-pore domain K+ channels TREK-2 and TRAAK. *J Physiol* **564**:103-116.

Kim Y, Bang H, Gnatenco C and Kim D (2001) Synergistic interaction and the role of C-terminus in the activation of TRAAK K+ channels by pressure, free fatty acids and alkali. *Pflugers Arch* **442**:64-72.

Downloaded from jpet.aspetjournals.org at ASPET Journals on March 13, 2024

JPET Fast Forward. Published on December 2, 2009 as DOI: 10.1124/jpet.109.162313
This article has not been copyedited and formatted. The final version may differ from this version.

Knot HJ and Nelson MT (1998) Regulation of arterial diameter and wall [Ca2+] in cerebral arteries of rat by membrane potential and intravascular pressure. *J Physiol* **508 (Pt 1)**:199-209.

Lesage F and Lazdunski M (2000) Molecular and functional properties of two-pore-domain potassium channels. *Am J Physiol Renal Physiol* **279**:F793-801.

Lesage F, Maingret F and Lazdunski M (2000) Cloning and expression of human TRAAK, a polyunsaturated fatty acids-activated and mechano-sensitive K(+) channel. *FEBS Lett* **471**:137-140.

Levine B, Park J, Smith TD and Caplan YH (1985) Chloral hydrate: unusually high concentrations in a fatal overdose. *J Anal Toxicol* **9**:232-233.

Lopes CM, Rohacs T, Czirjak G, Balla T, Enyedi P and Logothetis DE (2005) PIP2 hydrolysis underlies agonist-induced inhibition and regulates voltage gating of two-pore domain K+ channels. *J Physiol* **564**:117-129.

Lotshaw DP (2007) Biophysical, pharmacological, and functional characteristics of cloned and native mammalian two-pore domain K+ channels. *Cell Biochem Biophys* **47**:209-256.

Lowry JP and Fillenz M (2001) Real-time monitoring of brain energy metabolism in vivo using microelectrochemical sensors: the effects of anesthesia. *Bioelectrochemistry* **54**:39-47.

Maingret F, Fosset M, Lesage F, Lazdunski M and Honore E (1999) TRAAK is a mammalian neuronal mechano-gated K+ channel. *J Biol Chem* **274**:1381-1387.

Downloaded from jpet.aspetjournals.org at ASPET Journals on March 13, 2024

JPET Fast Forward. Published on December 2, 2009 as DOI: 10.1124/jpet.109.162313
This article has not been copyedited and formatted. The final version may differ from this version.

Marrelli SP, Eckmann MS and Hunte MS (2003) Role of endothelial intermediate conductance KCa channels in cerebral EDHF-mediated dilations. *Am J Physiol Heart Circ Physiol* **285**:H1590-1599.

Merdink JL, Robison LM, Stevens DK, Hu M, Parker JC and Bull RJ (2008) Kinetics of chloral hydrate and its metabolites in male human volunteers. *Toxicology* **245**:130-140.

Nelson MT and Quayle JM (1995) Physiological roles and properties of potassium channels in arterial smooth muscle. *Am J Physiol* **268**:C799-822.

NTP (2002) Toxicology and carcinogenesis study of chloral hydrate (ad libitum and dietary controlled) (CAS no. 302-17-0) in male B6C3F1 mice (gavage study). *Natl Toxicol Program Tech Rep Ser*:1-218.

Pershad J, Palmisano P and Nichols M (1999) Chloral hydrate: the good and the bad. *Pediatr Emerg Care* **15**:432-435.

Pochet S, Keskiner N, Fernandez M, Marino A, Chaib N, Dehaye JP and Metioui M (2002) Multiple effects of trichloroethanol on calcium handling in rat submandibular acinar cells. *Br J Pharmacol* **136**:568-580.

Reyes R, Lauritzen I, Lesage F, Ettaiche M, Fosset M and Lazdunski M (2000) Immunolocalization of the arachidonic acid and mechanosensitive baseline traak potassium channel in the nervous system. *Neuroscience* **95**:893-901.

Scheibler P, Kronfeld A, Illes P and Allgaier C (1999) Trichloroethanol impairs NMDA receptor function in rat mesencephalic and cortical neurones. *Eur J Pharmacol* **366**:R1-2.

Downloaded from jpet.aspetjournals.org at ASPET Journals on March 13, 2024

JPET Fast Forward. Published on December 2, 2009 as DOI: 10.1124/jpet.109.162313
This article has not been copyedited and formatted. The final version may differ from this version.

Silverman J and Muir WW, 3rd (1993) A review of laboratory animal anesthesia with chloral hydrate and chloralose. *Lab Anim Sci* **43**:210-216.

Twite MD, Rashid A, Zuk J and Friesen RH (2004) Sedation, analgesia, and neuromuscular blockade in the pediatric intensive care unit: survey of fellowship training programs. *Pediatr Crit Care Med* **5**:521-532.

Uematsu M, Takasawa M, Hosoi R and Inoue O (2009) Uncoupling of flow and metabolism by chloral hydrate: a rat in-vivo autoradiographic study. *Neuroreport* **20**:219-222.

Downloaded from jpet.aspetjournals.org at ASPET Journals on March 13, 2024

JPET Fast Forward. Published on December 2, 2009 as DOI: 10.1124/jpet.109.162313
This article has not been copyedited and formatted. The final version may differ from this version.

Footnotes

Financial Support: At BCM, this work was supported by National Institutes of Health (NIH) grants [P01 NS38660 and R01 NS46666 (to Dr. Bryan)], and [F32 HL080916-01 (to Dr. Andresen)]. At UMKC, this work was supported by American Heart Association (AHA) [SDG 0735053N] and School of Medicine start-up funds (to Dr. Andresen) as well as Sarah Morrison Research Awards (to Ms. Jansen and Mr. Vaughn).

Portions of this work were previously presented at Experimental Biology 2007 in Washington, DC April 28 - May 2 2007.

Authors N.P. and N.S. contributed equally to this work.

Reprint requests:

Jon Andresen, Ph.D.

Basic Medical Science Department

University of Missouri-Kansas City School of Medicine

2464 Charlotte St., HSB 2232

Kansas City, MO 64108

Office: 816-235-1883

Fax: 816-235-6517

andresenj@umkc.edu

Downloaded from jpet.aspetjournals.org at ASPET Journals on March 13, 2024

JPET Fast Forward. Published on December 2, 2009 as DOI: 10.1124/jpet.109.162313
This article has not been copyedited and formatted. The final version may differ from this version.

Legends for Figures

Figure 1. Dilation of the rat MCA to TCE. Top: Raw traces of arterial diameter. Bottom: Summary data. A) In the control condition (closed, black circles), denuded, pressurized and perfused rat MCAs dilated in response to increasing concentrations of TCE (N=5). B) Replacing the control Krebs buffer with a buffer containing isotonic 60 mM KCl (closed, dark grey squares) impaired ($p<0.0001$) the response to TCE (N=8). C) Inclusion of an inhibitory cocktail of classical K^+ channel blockers (open, light grey circles) did not alter the dilation caused by TCE (N=4). Summary data are means±SEM.

Figure 2. TRAAK protein expression. A) Western blot showing TRAAK immunopositive bands at 43 kDa in rat cardiovascular tissues. Cerebral arteries=MCA+basilar. Positive (+) control is IMR-32 human neuroblastoma cell lysate (Santa Cruz Biotechnology product sc-2409. B) Sections of rat brain and MCA imaged at three levels of magnification (10X, 40X, and 60X oil immersion) using epifluorescence microscopy. Tissue slices (8 μm) were incubated with a primary antibody directed towards TRAAK (right) or an equal amount of a control non-immune IgG (left). Red fluorescence is TRAAK and blue is DAPI staining of nuclei.

Figure 3. Electrophysiology of isolated rat MCA smooth muscle cells. Whole-cell patch clamp current recordings of freshly dissociated rat MCA smooth muscle cells. In response to a voltage step protocol (signal, -80 mV to 80 mV, 60 ms pulses separated by 10 mV) TCE elicited concentration-dependent increases in current (mostly in the outward

Downloaded from jpet.aspetjournals.org at ASPET Journals on March 13, 2024

JPET Fast Forward. Published on December 2, 2009 as DOI: 10.1124/jpet.109.162313
This article has not been copyedited and formatted. The final version may differ from this version.

direction) under control conditions (left) and after inhibition of classical K^+ channels with the IC (right). Note the difference in scale: Control is -400 to 3000 pA, and Inhibitory Cocktail is -400 to 500pA.

Figure 4. Summary data of currents activated by TCE in rat MCA smooth muscle cells. Entire figure: control cells (N=5 animals) are on the left, and cells treated with the IC of classical K^+ channel blockers (N=5 animals) are on the right. A) At 10^{-2} M, TCE increased peak outward current in both control cells and in cells treated with the IC. B&C) I-V curves of baseline currents are shown by black circles, open circles show currents stimulated by TCE at 10^{-3} M, and 10^{-2} M TCE by closed squares. B) Under control conditions, TCE increased whole-cell currents at both 10^{-3} M and 10^{-2} M. Inclusion of the IC reduced overall whole-cell currents and increases over baseline were only seen to 10^{-2} M TCE. C) Subtracting out the baseline responses generated difference currents representing the currents due only to TCE (I_{TCE}). Although the I_{TCE} was non-zero for both concentrations of TCE under control conditions, I_{TCE} at 10^{-2} M was greater than at 10^{-3} M. In the presence of the IC, however, only 10^{-2} M TCE was sufficient to generate currents that were non-zero, or different from baseline. Data are means±SEM. * indicates a statistically significant difference ($p \leq 0.05$).

Figure 5. Changes in reversal potential with increased extracellular potassium. Top: traces of an rat MCA smooth muscle cell treated with the IC of classical K^+ channel blockers and 10^{-2} M TCE as the extracellular K^+ concentration is raised from 5.4 mM to 54 and 140 mM. Bottom: Summary of experimental data collected from rat MCA smooth

Downloaded from jpet.aspetjournals.org at ASPET Journals on March 13, 2024

JPET Fast Forward. Published on December 2, 2009 as DOI: 10.1124/jpet.109.162313
This article has not been copyedited and formatted. The final version may differ from this version.

muscle cells (closed, red circles, N=4 animals), and simulated pure K^+ currents (solid, black squares). Regression lines were fitted to the experimental (red) and simulated (blue) data to determine the slope of the response. Solid lines=best-fit line, dashes=95% confidence interval of the best-fit line. Data are means±SEM. * indicates a statistically significant difference ($p \leq 0.05$).

Figure 6. Baseline response of rat MCA smooth muscles cell to heat. Whole-cell current traces of a MCA smooth muscle cell responding to a voltage ramp protocol (stimulus, -100 mV to +100 mV in 700 ms) in the presence of the IC to block classical K^+ channels. Heating the preparation from room temperature (22°C) to 33°C did not alter the baseline response of the cell.

Figure 7. Effect of heat on the TCE response in rat MCA smooth muscle cells. A) An example of a whole-cell voltage clamp recording of an isolated rat MCA smooth muscle cell treated with 10^{-3} M TCE in the presence of the IC to block classical K^+ channels. In response to a voltage step protocol (inset) currents at 33°C were augmented over those at room temperature (22°C). B) Summary data (N=5 animals) showing that I-V curves of MCA smooth muscles cells at room temperature (22°C) at baseline (solid circles), and after addition of 10^{-3} M TCE (open circles) were similar, but that simply heating to 33°C (solid squares) enhanced the currents. C) Summary of peak outward currents at room temperature and at 33°C in the presence of the IC and 10^{-3} M TCE. D) Subtracting out the baseline I-V response revealed that the currents attributable to 10^{-3} M TCE ($I_{TCE\ (-3)}$) at 33°C were greater than zero, meaning that they were different than the baseline

Downloaded from jpet.aspetjournals.org at ASPET Journals on March 13, 2024

JPET Fast Forward. Published on December 2, 2009 as DOI: 10.1124/jpet.109.162313
This article has not been copyedited and formatted. The final version may differ from this version.

currents. E) I-V plot of difference currents due to 10^{-2} M TCE at room temperature ($I_{TCE\ (-2)\ RT}$, open circles) and to 10^{-3} M TCE at 33°C ($I_{TCE\ (-3)\ 33°}$, closed circles). Data are means±SEM. * indicates a statistically significant difference ($p \leq 0.05$).

Downloaded from jpet.aspetjournals.org at ASPET Journals on March 13, 2024

Figure 1

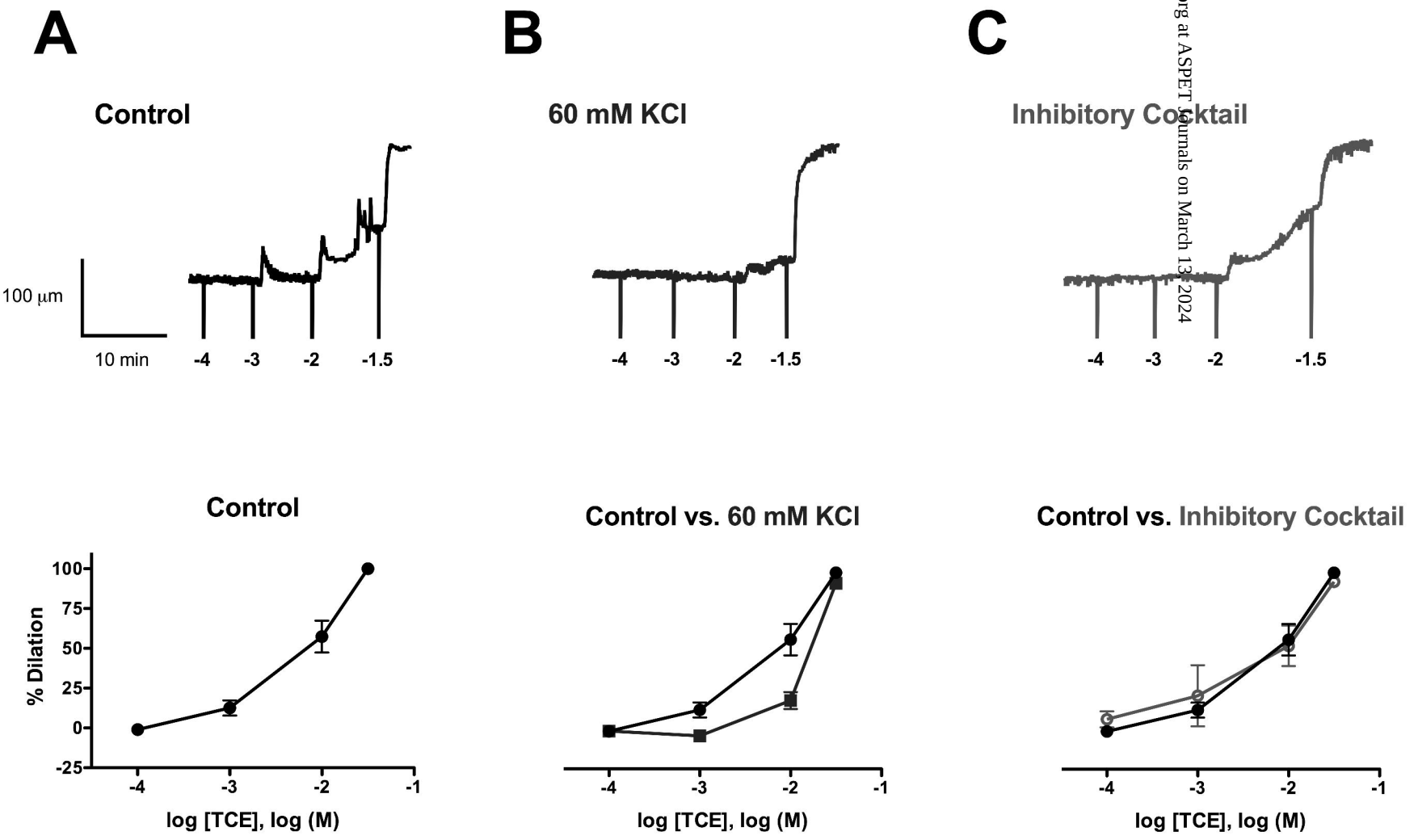

from jpet.aspetjournals.org at ASPET Journals on March 13, 2024

Figure 2

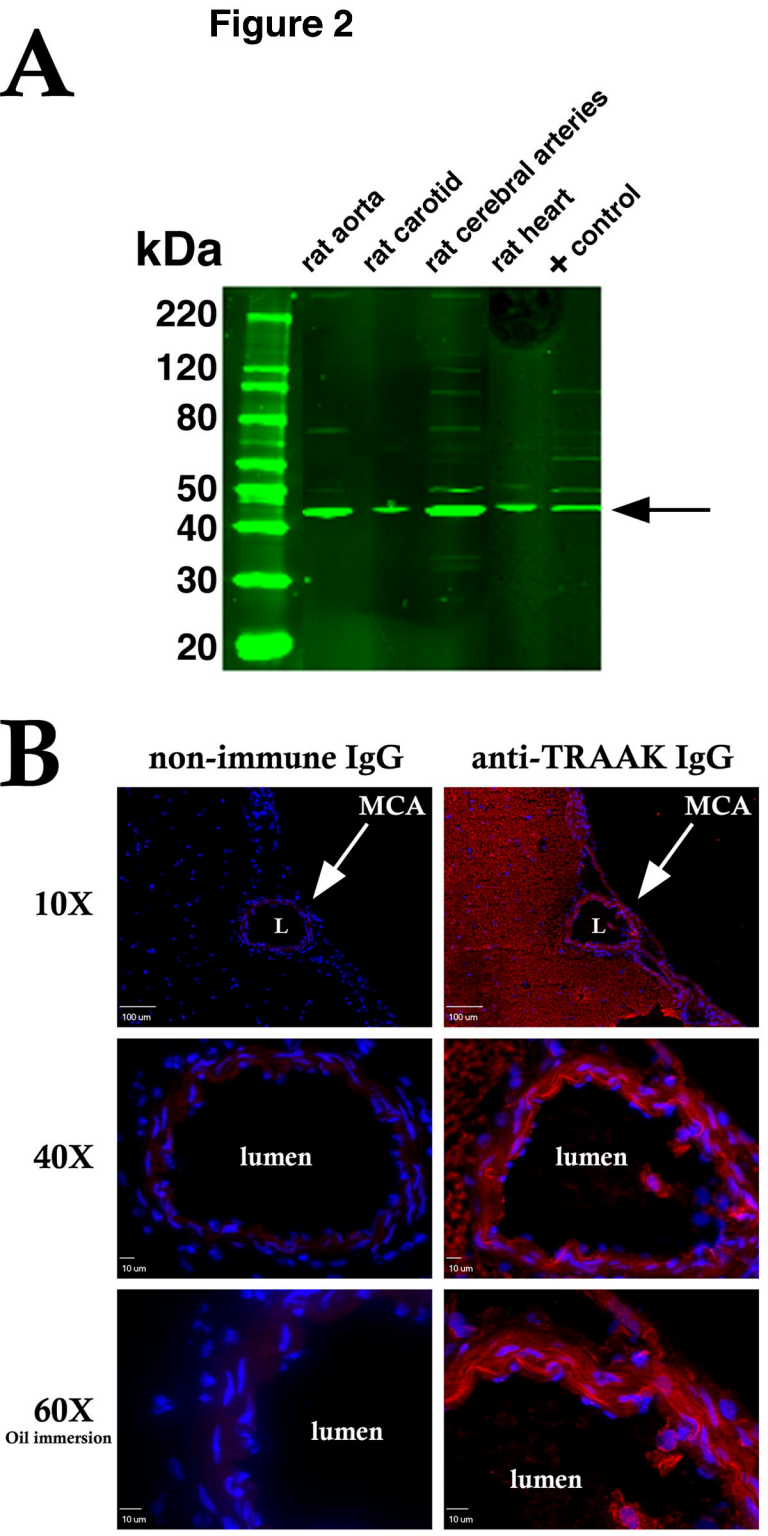
A
kDa
rat aorta
rat carotid
rat cerebral arteries
rat heart
+ control
220
120
80
50
40
30
20
B
non-immune IgG
anti-TRAAK IgG
10X
MCA
L
100 um
40X
lumen
10 um
60X
Oil immersion

Figure 3

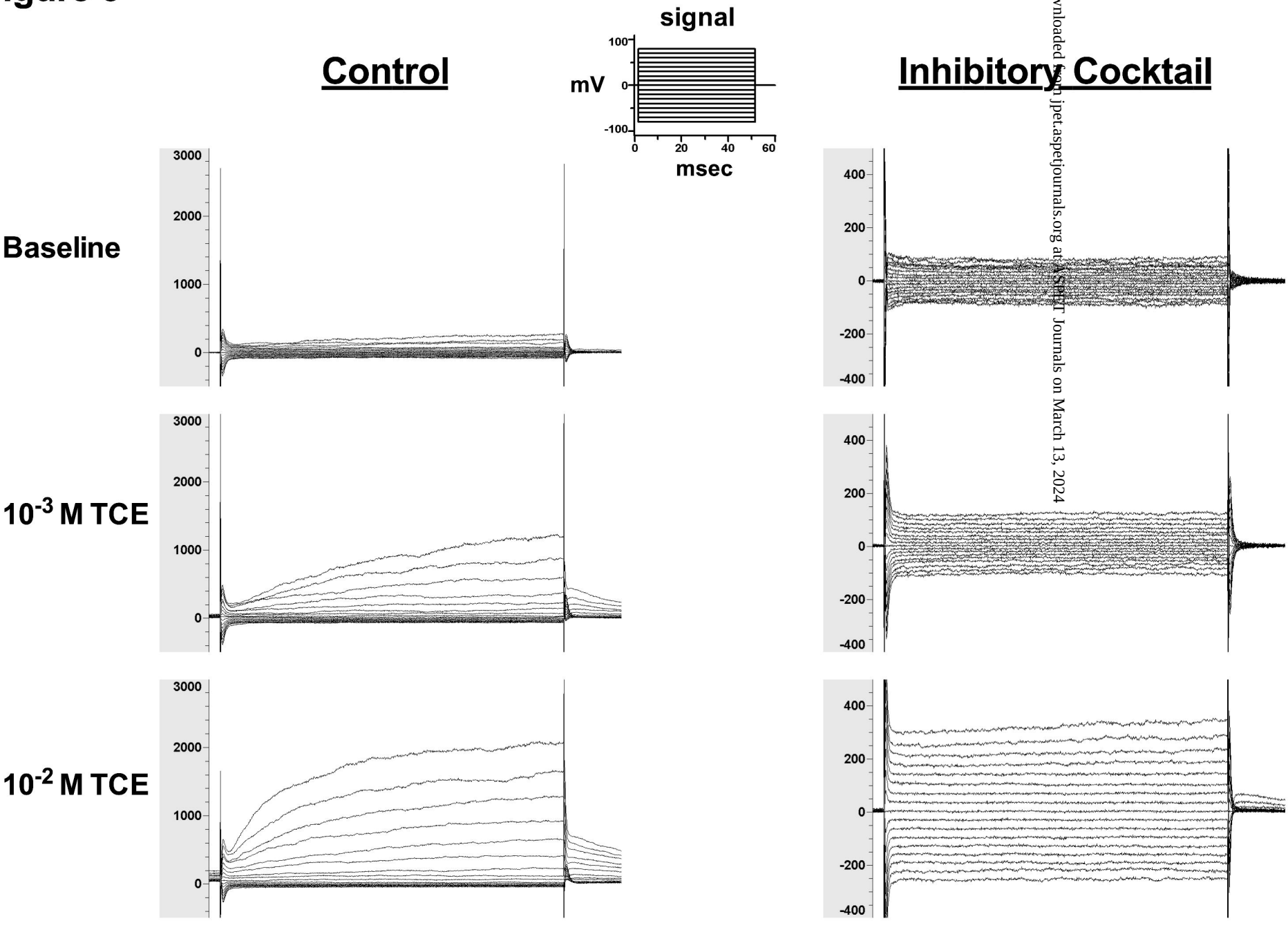

Downloaded from jpet.aspetjournals.org at ASPET Journals on March 13, 2024

Figure 4

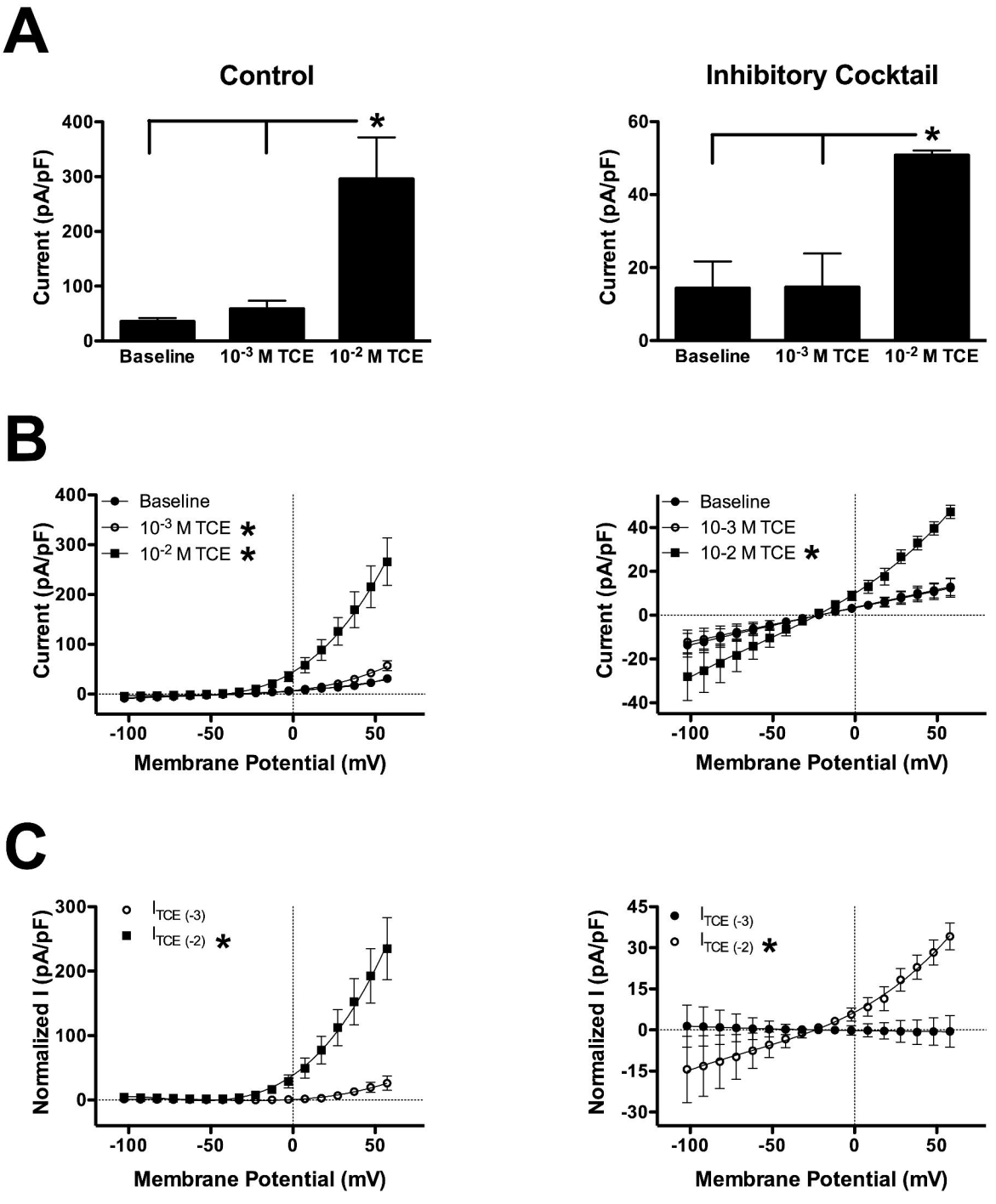
A
Control
Inhibitory Cocktail
Current (pA/pF)
400
300
200
100
0
60
40
20
*
Baseline
10-3 M TCE
10-2 M TCE
B
Baseline
10-3 M TCE *
10-2 M TCE *
10-3 M TCE
10-2 M TCE *
-100
-50
0
50
Membrane Potential (mV)
C
Normalized I (pA/pF)
300
200
100
45
30
15
-15
-30
ITCE (-3)
ITCE (-2) *

Figure 5

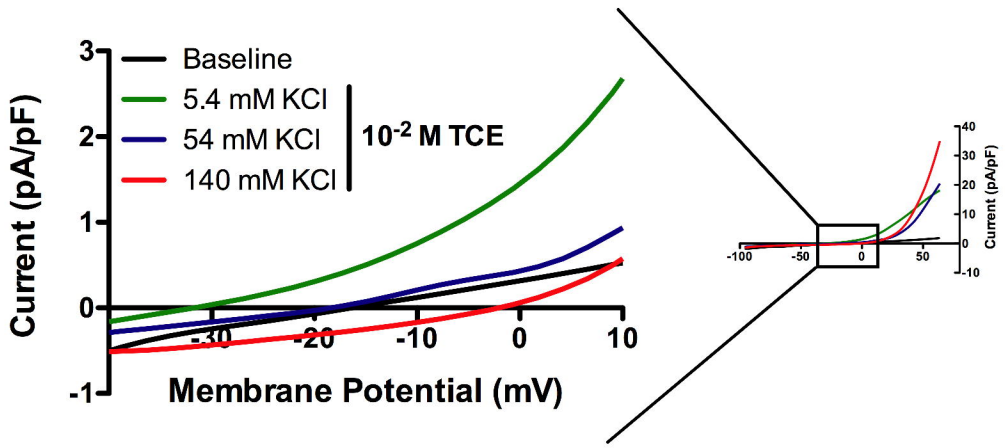

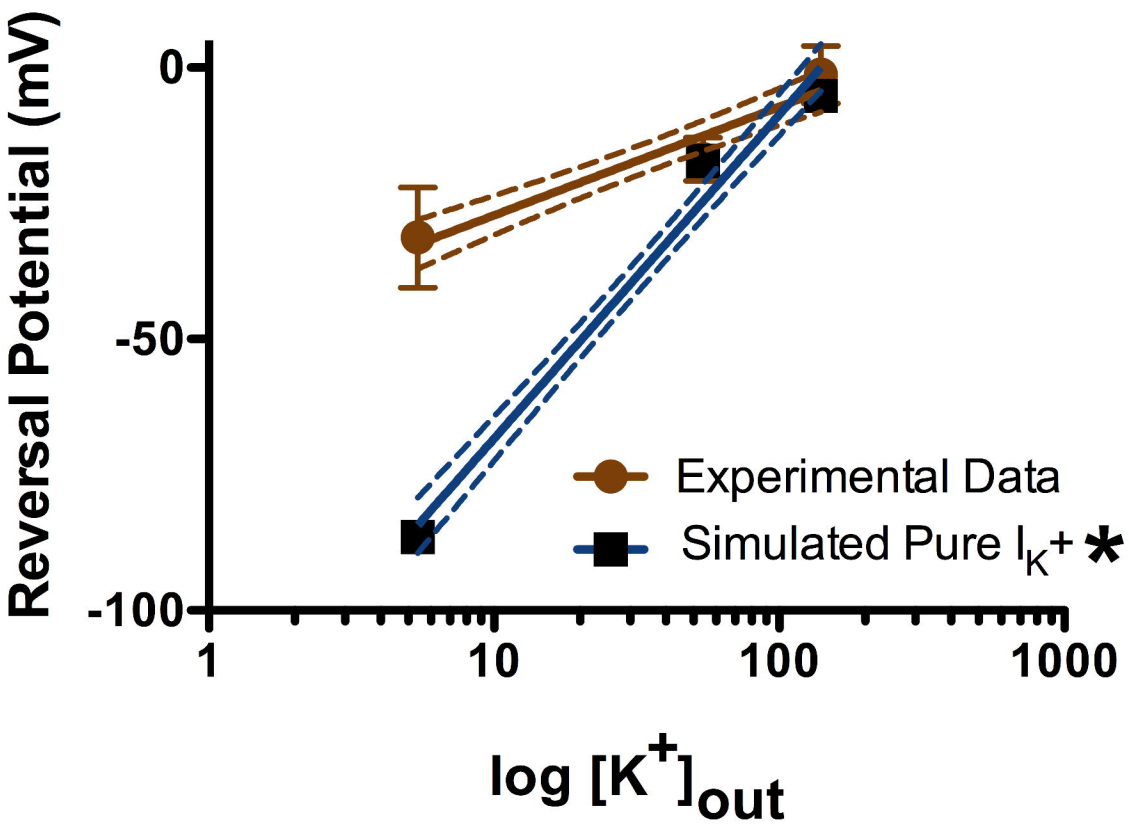

	Experimental Data	Simulated Pure I_K+
Slope	19.98	59.65

Figure 6

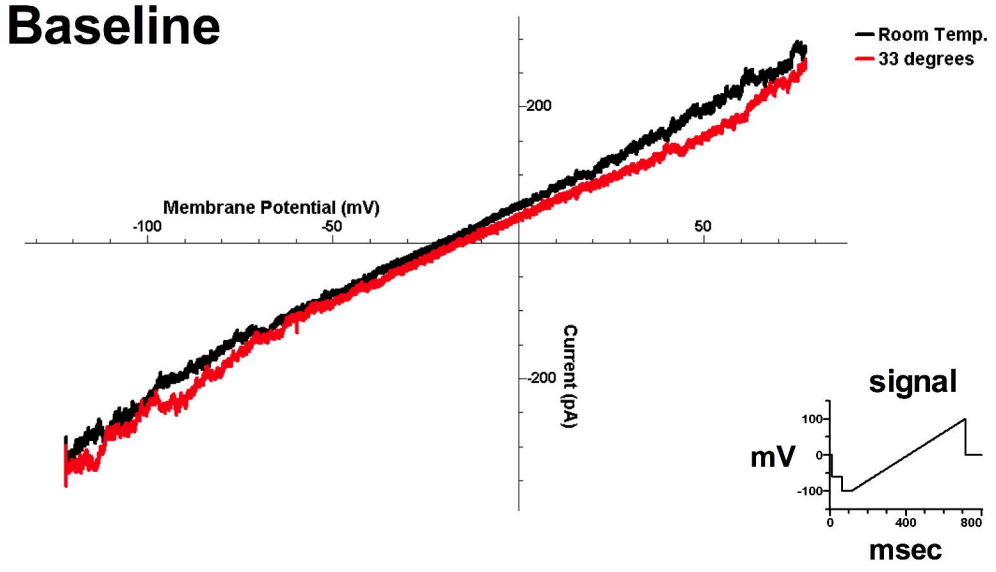
Baseline
Room Temp.
33 degrees
200
Membrane Potential (mV)
-100
-50
50
-200
Current (pA)
signal
100
mV
0
-100
0
400
800
msec

Figure 7

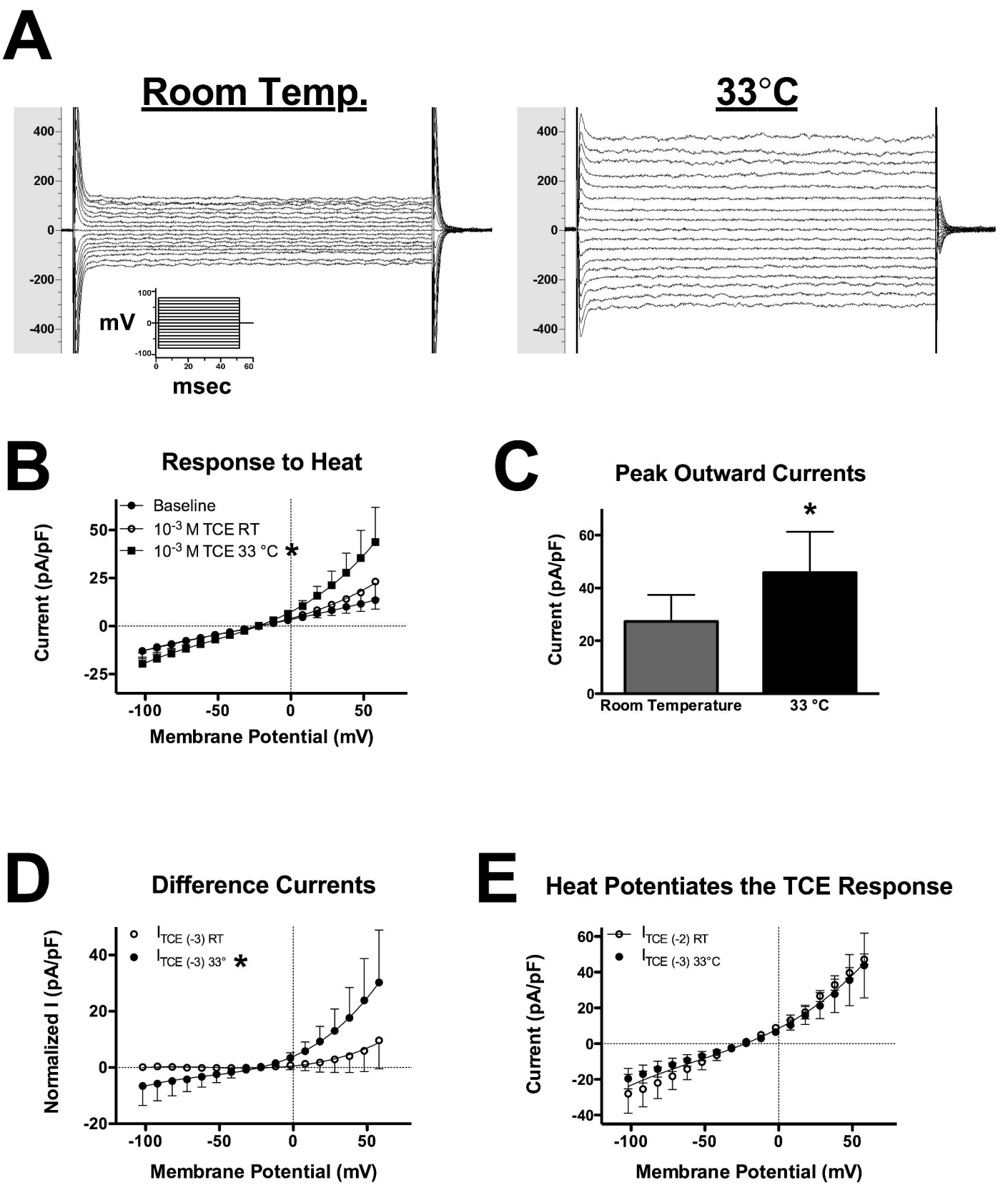
A
Room Temp.
33°C
400
200
0
-200
-400
mV
100
0
-100
0
20
40
60
msec
B
Response to Heat
Baseline
10-3 M TCE RT
10-3 M TCE 33 °C
*
Current (pA/pF)
50
25
0
-25
-100
-50
0
50
Membrane Potential (mV)
C
Peak Outward Currents
*
Current (pA/pF)
60
40
20
0
Room Temperature
33 °C
D
Difference Currents
ITCE (-3) RT
ITCE (-3) 33°
*
Normalized I (pA/pF)
40
20
0
-20
-100
-50
0
50
Membrane Potential (mV)
E
Heat Potentiates the TCE Response
ITCE (-2) RT
ITCE (-3) 33°C
Current (pA/pF)
60
40
20
0
-20
-40
-100
-50
0
50
Membrane Potential (mV)